Chapter 3

Weak discontinuities in one-dimensional compressible non-ideal gas dynamics *

"We cannot solve our problems with the same thinking we used when we created them."

–Albert Einstein

*"The contents of this chapter have been published in ***Zeitschrift für Naturforschung A (De Gruyter), 2022."***

3.1 Introduction

In this chapter, we investigated the various parameter effects on the propagation of weak discontinuities by using the method of characteristics. We obtained the analytical solutions of the quasi-linear system of hyperbolic PDEs and examined the evolutionary behavior of shock in the characteristic plane. Nonlinearity in PDEs is a significant challenge for any mathematical or physical problem involving a partial differential equation. There is no standard procedure for determining the solution of non-linear PDEs. When we look at the system of the partial differential equation, the problem becomes more complicated. Finding an analytical solution for the non-linear system and study the wave propagation phenomena associated with this system is still a broad area of research. Some well-known methods for solving non-linear PDEs have been developed in the past, such as the method of characteristics, perturbation method, wavefront analysis, progressive wave solution, self-similar solutions, differential transform method [1, 2, 90]. These are the methods used to investigate non-linear PDEs and the non-linear waves described by these systems.

Over the past few decades, many researchers analyzed the theory of weak discontinuities in different gaseous media such as ideal gas dynamics, magnetogasdynamics, dusty gas dynamics, etc [57, 87, 91]. It has a wide range of applications in numerous fields like plasma physics, astrophysics, nuclear physics, space science. Green [92] examined the evolutionary behavior of plane discontinuities in elastic materials and observed that the discontinuity of higher order remains unchanged whereas the second order discontinuity (acceleration discontinuity) becomes shock in finite time or it gradually decays and ended in infinite time. Weak discontinuities are the discontinuities that occur in the solution's derivative along with the characteristics, whereas the solution itself remains continuous. Ram [55] have studied the evolutionary process of acceleration discontinuities and determined the condition

for shock formation. Sharma and Shyam [93] examined the radiative transfer effects on the growth and decay of weak discontinuities in three-dimensional inviscid gas flow. Sharma and Arora [94] have studied the interaction of acceleration waves with characteristic shock in interstellar gas clouds.

When we encounter weak discontinuities in different material mediums, we see that the amplitudes of these discontinuities always obey the same differential equation. If X denotes the amplitudes of the discontinuity, then X obeys the following differential equation.

$$\frac{dX}{dt} = -\tau X + \kappa X^2, \quad 0 \leq t < \infty,$$

here t is the time. In general, the coefficients τ and κ are the functions of t. The above equation is the well-known Bernoulli equation. The entire study of the flow profile of the weak discontinuities depends on the solution of the Bernoulli Equation. Since we can obtain precisely the amplitude of the weak discontinuity without any approximations, even though we deal with an utterly non-linear theory, we believe this is the main reason why weak discontinuities are especially useful. In this paper, we used the method of characteristics to find the analytical solution of the hyperbolic system of the partial differential equation and explore the nature of propagating waves in van der Waals dusty medium for planar and cylindrically symmetric flow.

For many years, shock wave theory has been used in several scientific and industrial domains for experimental and research purposes [95, 96]. The formation of shock waves, which are rapid changes in pressure, density, and velocity, is the most notable phenomenon in the nonlinear theory. Shock phenomena occur in many astrophysical supersonic flows with an associated angular momentum leading to the flow become subsonic flow. This happens because such flows encounter a powerful centrifugal potential barrier that breaks the motion, and the stationary solution can only be introduced through shock. In stellar environments, shock waves,

such as those produced by a core-collapse supernova explosion, are transformed into radiation-mediated shocks. Such shocks form when photons collide with matter's electrons, and the downstream of these shocks is dominated by radiation energy density rather than thermal energy density [97]. The relativistic shock wave is a particular example of an astrophysical shock wave, in which the velocity of the shock is the non-negligible fraction of the speed of light. Shock formation in black hole accretion is also expected to be a general phenomenon because shock waves in rotating and non-rotating flows are convincingly capable of converting a significant amount of gravitational energy [98, 99]. Das [100] explored the possibility of shock formation in black hole accretion discs and observed that standing shocks are a crucial component of accretion discs near non-rotating black holes in general.

We consider the following quasilinear hyperbolic system of PDEs governing the one-dimensional compressible flow of van der Waals gas with small solid particles as [101]

$$\begin{cases} \dfrac{\partial \rho}{\partial t} + u\dfrac{\partial \rho}{\partial x} + \rho\dfrac{\partial u}{\partial x} + \dfrac{m\rho u}{x} = 0, \\ \rho\left(\dfrac{\partial u}{\partial t} + u\dfrac{\partial u}{\partial x}\right) + \dfrac{\partial p}{\partial x} = 0, \\ \dfrac{\partial E}{\partial t} + u\dfrac{\partial E}{\partial x} - \dfrac{p}{\rho^2}\left(\dfrac{\partial \rho}{\partial t} + u\dfrac{\partial \rho}{\partial x}\right) = 0, \end{cases} \tag{3.1}$$

where ρ, p and u are the density, pressure and the velocity along the x-axis, respectively. Here x represents the spatial coordinate and t is the time. Here $m = 0, 1, 2$ for planar, cylindrical and spherical symmetry respectively. The internal energy E per unit mass of the mixture can be written as

$$E = \frac{(1 - Z)(1 - \tilde{b}\rho)p}{(\Gamma - 1)\rho}. \tag{3.2}$$

where $Z = V_{sp}/V_g$ is the volume fraction of the solid particles. V_{sp} denotes the volume of the solid particles and V_g denotes the entire volume of the mixture; $\tilde{b} = b(1 - k_p)$ where b is the parameter of non-idealness. The Grüneisen coefficient Γ is given by

$$\Gamma = \frac{\gamma(1 + \lambda\beta)}{(1 + \lambda\beta\gamma)},$$

where $\lambda = k_p/(1 - k_p)$, $\beta = c_{sp}/c_p$, $\gamma = c_p/c_v$. The parameter c_{sp} denotes the specific heat of solid particles, c_p and c_v denote the specific heat of the gas at constant pressure and at constant volume, respectively. Here $k_p = m_{sp}/m_g$ is the mass fraction of dust particles, where m_{sp} and m_g are the mass of the dust particles and total mass of the mixture respectively. The volume fraction Z and mass fraction k_p are related by $Z = \theta\rho$, $\theta = k_p/\rho_{sp}$, where ρ_{sp} is the specific density of the dust particles.

Study of fluid flow containing small solid particles play an important role in the field of fluid dynamics from a mathematical and physical point of view [15, 102, 103, 104, 105, 106, 107]. Explosive volcano eruptions, interstellar masses, and subsurface explosions are examples of fluid mixing solid particles, an essential topic in mathematics and physics [108, 109, 110]. A dusty gas is a mixture of micro-sized solid particles and gas, in which the particle volume only contributes a small percentage of the mixture's total volume. Miura [14] has presented a numerical analysis of the unsteady nonequilibrium flow of dusty gas in a shock tube, where the particle cloud's drag and heat transfer rate are computed for a single particle using a semi-empirical technique. Pang et al.[111], Chaudhary and Singh [112] have discussed the properties of elementary waves of the Riemann problem in dusty gasdynamics. In addition, Chaturvedi and Singh [113] used the two-parameter flux approximation to examine the concentration and cavitation phenomenon in the solution of the Riemann problem to the pressureless isentropic Euler equations for the dusty gas flow. Higashino

[114] investigated the problem of blast waves in a dusty medium and addressed how dust particles affect blast wave decay. He discovered that when the volume fraction of dust particles grows, the material density at the shock front assembles, and the pressure and velocity profiles' slopes increase. Gupta et al.[115] further presented the wave interaction phenomena in dusty gas regime by using the multiple time scale method. Laibe and Price [116] investigated the formulation of the basic equations describing the flow of a dusty gas mixture and its properties. They reformulated the governing equations of dusty gas flow to a single fluid moving with the barycenter of the mixture and determined a set of equations that are only slightly different from the usual equations of gas dynamics, with an extra evolution equation describing the differential velocity and the ratio of dust and gas in the mixture.

The equation of state is given by

$$p = \frac{(1 - k_p)}{(1 - Z)(1 - \tilde{b}\rho)} \rho R T, \tag{3.3}$$

where R is the specific gas constant and T is the temperature of the gas and that of solid particles.

The complete summary of this chapter is organized as follows: In the second section, we obtain the governing equation modeled in non-ideal gas with small solid particles and determine the characteristic curves representing the wave propagation. We introduce the characteristic variables and transform the fundamental equation in terms of characteristic variables. In the next section, we derive a differential equation and its solution to investigate the evolution process of weak discontinuities. In the fourth section, we analyzed the behavior of the solution of the growth equation and determined the variation of the curves representing the solution with the various parameters of the flow. The discussion of the different parameter effects on the shock formation and distortion process is the subject of the result and discussion

section. The conclusion of this chapter's comprehensive analysis is presented in the final part.

3.2 Characteristic Transformation

On insertion of equations (3.2) and (3.3) in (3.1), and neglecting the terms containing $\mathcal{O}(b^2)$, system (3.1) can be rewritten into the following form

$$\begin{cases} \dfrac{\partial \rho}{\partial t} + u\dfrac{\partial \rho}{\partial x} + \rho\dfrac{\partial u}{\partial x} + \dfrac{m\rho u}{x} = 0, \\ \dfrac{\partial u}{\partial t} + u\dfrac{\partial u}{\partial x} + \dfrac{1}{\rho}\dfrac{\partial p}{\partial x} = 0, \\ \dfrac{\partial p}{\partial t} + u\dfrac{\partial p}{\partial x} + \rho a^2\left(\dfrac{\partial u}{\partial x} + \dfrac{mu}{x}\right) = 0, \end{cases} \tag{3.4}$$

where a is the speed of sound given as

$$a^2 = \frac{(\Gamma - \sigma_2\rho^2)p}{(1 - \sigma_1\rho + \sigma_2\rho^2)\rho},$$

where $\sigma_1 = \theta + \tilde{b}$ and $\sigma_2 = \theta\tilde{b}$.

Now we discuss the cases based on the parameter θ and b, which determine the medium of the flow.

Case 1: $\theta = 0$ corresponds to the non-ideal gas flow without dust particles. In this case, $\Gamma = \gamma$ and $a^2 = \frac{\gamma p}{(1-b\rho)\rho}$.

Case 2: If θ and b both are zero, then $\Gamma = \gamma$, $a^2 = \frac{\gamma p}{\rho}$, and the medium becomes non-dusty ideal gas flow.

Case 3: If $b = 0$, then $\Gamma \neq \gamma$ and speed of sound is given by $a^2 = \frac{\Gamma p}{(1-Z)\rho}$, and the flow becomes ideal gas flow with dust particles.

Case 4: If θ and b both are non-zero, in this case $\Gamma \neq \gamma$, $a^2 = \frac{(\Gamma-\sigma_2\rho^2)p}{(1-\sigma_1\rho+\sigma_2\rho^2)\rho}$, and the

flow becomes non-ideal dusty gas flow.

Equation (3.4) can be written as

$$U_t + AU_x + B = 0, \tag{3.5}$$

where

$$A = \begin{pmatrix} u & \rho & 0 \\ 0 & u & \rho^{-1} \\ 0 & \rho a^2 & u \end{pmatrix}, \quad U = \begin{pmatrix} \rho \\ u \\ p \end{pmatrix}, \quad \text{and} \quad B = \begin{pmatrix} \frac{m\rho u}{x} \\ 0 \\ \frac{m\rho a^2 u}{x} \end{pmatrix}. \tag{3.6}$$

Here, the function $U(x,t)$ satisfying (3.5) everywhere except for the characteristic curve S(t), where U is continuous, but U_t and U_x experiences finite jump. Denoting the jump of a quantity U across $S(t)$ by [U], we have along $S(t)$

$$\frac{\partial}{\partial t}[U] = [U_t] + \frac{dS(t)}{dt}[U_x], \tag{3.7}$$

where $\dfrac{\partial}{\partial t}$ denotes the partial derivative with respect to time t.

Since, it is given that U is a continuous everywhere, therefore $[U] = 0$.

In view of (3.7) and the continuity condition $[U] = 0$, jump in (3.5) can be written as

$$\left(A - \frac{dS}{dt}I\right)[U_x] = 0. \tag{3.8}$$

Here, I is the identity matrix of order 3. Equation (3.8) shows that the characteristic speed of propagation $\dfrac{dS}{dt}$ of the discontinuity is an eigenvalue of A. It follows that (3.5) has three families of characteristic curves, which are given by

$$\frac{dx}{dt} = u \pm a, \tag{3.9}$$

represents the discontinuity propagating in $\pm x$-direction with local speed a, and the remaining characteristic curve is

$$\frac{dx}{dt} = u, \tag{3.10}$$

represents the particle path.

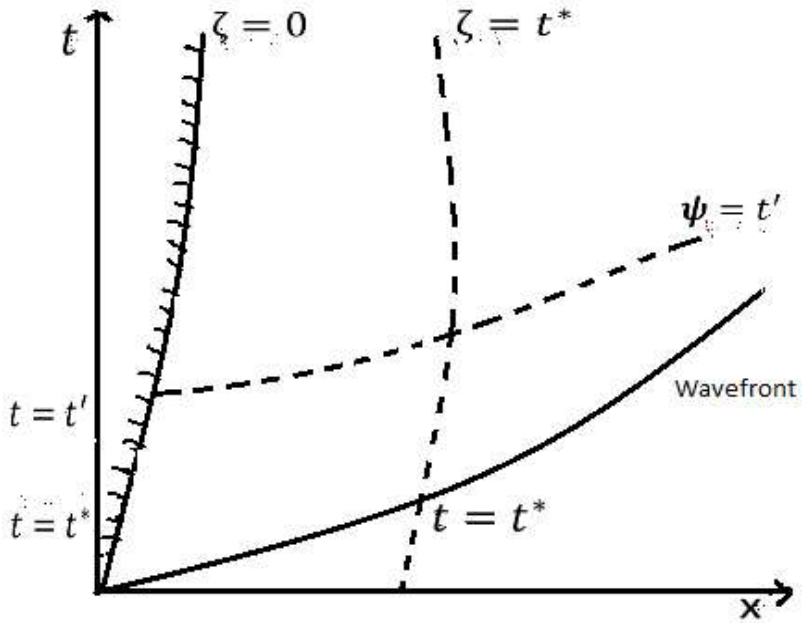

FIGURE 3.1: Characteristic labeling and coordinate system.

When dealing with the hyperbolic system of PDEs, using the characteristic variable as a reference coordinate will be more convenient. We introduce characteristic variables ζ and ψ, where ζ is chosen in such a way that it represents the particle tag and constant along the particle path $\frac{dx}{dt} = u$. ψ represents the wave tag and it is constant along the outgoing characteristic $\frac{dx}{dt} = u+a$ in (x,t) plane. The phenomena of characteristic transformation is shown by Fig.3.1. If the characteristic wave front traverses a particle at time t^*, this particle and its path will be labeled by $\zeta = t^*$. If an outgoing discontinuity (wave) is propagated at time $t^{'}$, then it will be labelled by $\psi = t^{'}$. Thus, it can be seen that for each pair (ψ, ζ), there is a corresponding pair (x,t) so that $x = x(\psi,\zeta)$, $t = t(\psi,\zeta)$. Now, the characteristic variables ψ and

ζ satisfy the following conditions

$$x_\psi = ut_\psi, \qquad x_\zeta = (u+a)t_\zeta. \tag{3.11}$$

Now, U_t and U_x takes the following form

$$U_t = \frac{U_\zeta x_\psi - U_\psi x_\zeta}{J}, \qquad U_x = \frac{U_\psi t_\zeta - U_\zeta t_\psi}{J}. \tag{3.12}$$

The Jacobian of the transformation is given by $J = \frac{\partial(x,t)}{\partial(\psi,\zeta)} = -at_\psi t_\zeta$, which plays a crucial role in solving the shock formation problem. Since physical considerations do not allow the overlapping of fluid particles, therefore, t_ζ can not be zero. As a result, when two neighboring characteristics combine to form a shock wave, $J = 0$ if and only if $t_\psi = 0$. Hence $J = 0$ gives the condition for the shock formation.

With the help of equation (3.12), (3.4) is transformed as

$$a\rho_\psi t_\zeta - \rho\left(u_\psi t_\zeta - u_\zeta t_\psi - \frac{muat_\psi t_\zeta}{x}\right) = 0, \tag{3.13}$$

$$\rho a u_\psi t_\zeta - p_\psi t_\zeta + p_\zeta t_\psi = 0, \tag{3.14}$$

$$ap_\psi t_\zeta - \rho a^2\left(u_\psi t_\zeta - u_\zeta t_\psi - \frac{muat_\psi t_\zeta}{x}\right) = 0. \tag{3.15}$$

Using (3.14) and (3.15) in (3.13), we obtain

$$p_\zeta + \rho a u_\zeta + \frac{m\rho u a^2 t_\zeta}{x} = 0. \tag{3.16}$$

The subscripts ζ and ψ denotes the partial derivatives with respect to ζ and ψ, respectively.

The boundary conditions at the wave front $\psi = 0$ are

$$[u] = 0, \;\; [\rho] = 0, \;\; [p] = 0, \;\; t = \zeta \quad . \tag{3.17}$$

Since the gas flow ahead of the discontinuity is homogeneous and at rest, therefore (3.17) requires

$$\rho_\zeta = 0, \;\; p_\zeta = 0, \;\; u_\zeta = 0 \;\text{ and }\; t_\zeta = 1 \quad \text{at } \; \psi = 0. \tag{3.18}$$

Using (3.17) and (3.18) in (3.14) and (3.11) and evaluating at the wave front $\psi = 0$, we obtain

$$p_\psi = \rho_0 a_0 u_\psi, \tag{3.19}$$

$$x_\psi = 0, \quad x_\zeta = a_0. \tag{3.20}$$

Here the flow variables evaluated ahead of the shock are signified by the subscript '0'. Using (3.18) in (3.12), we get

$$\left[\frac{\partial u}{\partial x}\right] = Y = -\frac{u_\psi}{a_0 t_\psi}, \quad \text{at } \; \psi = 0, \tag{3.21}$$

where Y represents the amplitude of the weak discontinuity at $\psi = 0$.

3.3 Evolution of amplitude of the discontinuity

In this section, we establish the conditions for the dependence of u_ψ and t_ψ on time. Differentiating equation (3.11), (3.16) and (3.19) with respect to ψ and ζ respectively, at $\psi = 0$, we get

$$\frac{u_{\psi\zeta}}{t_\psi} = \frac{m a_0}{2\zeta} Y, \tag{3.22}$$

$$\frac{t_{\psi\zeta}}{t_\psi} = \left\{ \frac{\Gamma + 1 - 2\sigma_2 \rho_0^2}{2(1 - \sigma_1 \rho_0 + \sigma_2 \rho_0^2)} - \frac{\sigma_2 \rho_0^2}{(\Gamma - \sigma_2 \rho_0^2)} \right\} Y. \tag{3.23}$$

Taking derivative of (3.21) with respect to ζ and using (3.22) and (3.23), we obtain

$$\frac{dY}{d\zeta} + \frac{m}{2\zeta}Y + \left\{ \frac{\Gamma + 1 - 2\sigma_2\rho_0^2}{2(1 - \sigma_1\rho_0 + \sigma_2\rho_0^2)} - \frac{\sigma_2\rho_0^2}{(\Gamma - \sigma_2\rho_0^2)} \right\} Y^2 = 0, \tag{3.24}$$

at $\psi = 0$. Now, we define the following dimensionless parameters given as

$$\eta = \frac{Y}{Y^*}, \;\; \mu = \frac{\zeta - \zeta^*}{2\zeta^*} \;\text{ and }\; \delta = Y^*\zeta^*, \tag{3.25}$$

where η is the wave amplitude, δ represents the initial acceleration and μ denotes the time in non-dimensional form. The superscript '*'used to denote the values of the variables at $t = t^*$.

Writing (3.24) in terms of non-dimensional parameters, we have

$$\frac{d\eta}{d\mu} + \frac{m}{2\mu + 1}\eta + \left\{ \frac{\Gamma + 1 - 2\sigma_2\rho_0^2}{(1 - \sigma_1\rho_0 + \sigma_2\rho_0^2)} - \frac{2\sigma_2\rho_0^2}{(\Gamma - \sigma_2\rho_0^2)} \right\} \delta\eta^2 = 0, \tag{3.26}$$

at $\psi = 0$.

Equation (3.26) is a Bernoulli type differential equation with η as a dependent variable and μ is an independent variable which can be solved by reducing it into linear differential equation and the analytical solution of eq.(3.26) is given as

$$\eta = \left\{ (2\mu + 1)^{\frac{m}{2}} \left(1 + \left(\frac{\Gamma + 1 - 2\sigma_2\rho_0^2}{(1 - \sigma_1\rho_0 + \sigma_2\rho_0^2)} - \frac{2\sigma_2\rho_0^2}{(\Gamma - \sigma_2\rho_0^2)} \right) \frac{\delta(2\mu + 1)^{1 - \frac{m}{2}}}{2(1 - \frac{m}{2})} \right) \right\}^{-1}. \tag{3.27}$$

In view of Eqs. (3.21) and (3.27), we see that $t_\psi = 0$ is the necessary condition for shock formation, therefore we must have $t_\psi = 0$, i.e.

$$1 + \left(\frac{\Gamma + 1 - 2\sigma_2\rho_0^2}{(1 - \sigma_1\rho_0 + \sigma_2\rho_0^2)} - \frac{2\sigma_2\rho_0^2}{(\Gamma - \sigma_2\rho_0^2)} \right) \frac{\delta(2\mu + 1)^{1 - \frac{m}{2}}}{2(1 - \frac{m}{2})} = 0. \tag{3.28}$$

The Condition (3.28) shows that only compressive weak discontinuities ($\delta < 0$) forms shock wave.

3.4 Behavior of Weak Discontinuities

Now we shall discuss some specific cases to investigate the possibilities of shock formation.

Case I. Planar flow :

In this case $m = 0$ and hence we have

$$\eta = \left\{1 + \left(\frac{\Gamma + 1 - 2\sigma_2\rho_0^2}{(1 - \sigma_1\rho_0 + \sigma_2\rho_0^2)} - \frac{2\sigma_2\rho_0^2}{(\Gamma - \sigma_2\rho_0^2)}\right)\frac{\delta(2\mu+1)}{2}\right\}^{-1}, \tag{3.29}$$

which implies that

$$Y = \frac{Y^*}{\left\{1 + \left(\frac{\Gamma+1-2\sigma_2\rho_0^2}{(1-\sigma_1\rho_0+\sigma_2\rho_0^2)} - \frac{2\sigma_2\rho_0^2}{(\Gamma-\sigma_2\rho_0^2)}\right)\frac{\delta(2\mu+1)}{2}\right\}}. \tag{3.30}$$

It can be seen from equation (3.30) that the amplitude of the expansive weak discontinuities ($\delta > 0$) decays and ultimately end up.

Case II. Non-Planar flow :

Cylindrically symmetric flow

Putting ($m = 1$) in (3.27), we obtain

$$\eta = \left\{(2\mu+1)^{\frac{1}{2}}\left(1 + \left(\frac{\Gamma + 1 - 2\sigma_2\rho_0^2}{(1 - \sigma_1\rho_0 + \sigma_2\rho_0^2)} - \frac{2\sigma_2\rho_0^2}{(\Gamma - \sigma_2\rho_0^2)}\right)\delta(2\mu+1)^{\frac{1}{2}}\right)\right\}^{-1}. \tag{3.31}$$

Using equation (3.31) in (3.25), the solution of the differential equation (3.26) can be written in the following form

$$Y = \frac{Y^*}{(2\mu+1)^{\frac{1}{2}}\left(1 + \left(\frac{\Gamma+1-2\sigma_2\rho_0^2}{(1-\sigma_1\rho_0+\sigma_2\rho_0^2)} - \frac{2\sigma_2\rho_0^2}{(\Gamma-\sigma_2\rho_0^2)}\right)\delta(2\mu+1)^{\frac{1}{2}}\right)}. \tag{3.32}$$

Equation (3.32) shows that the flattening of expansive weak discontinuities in cylindrically symmetric flow has a similar pattern as in the case of planar flow.

Spherically symmetric flow (m=2)

Substituting $m = 2$ in equation (3.27), we have $\eta = 0$, i.e. for the spherically symmetric flow, the amplitude of discontinuities vanishes. Therefore, for the spherically symmetric flow, equation (3.26) have trivial solution.

3.5 Results and Discussion

In the present investigation, we discuss the propagation of weak discontinuities in van der Waals gas with small solid dust particles for planar and non-planar ($m = 1$) flows. In the case of $m = 2$, we found that only a trivial solution is possible. Thus, the entire examination is discussed only for planar flow and non-planar flow for $m = 1$. We analyze the evolution of weak discontinuities and discuss the variation of flow patterns of the solution curves which relies on the values of the parameter of non-idealness and the mass fraction. Also, we examine the solution curves' steepening and flattening, representing the weak discontinuities with the increase in time. Also, we discuss when these discontinuities become shock waves and when they ended and the changes performed by increasing and decreasing the values of the parameters. The solution curves for positive values of δ represents the expansive weak discontinuities ($\delta > 0$) and negative values of δ represents the compressive weak discontinuities ($\delta < 0$).

Fig.3.2 presents the flow patterns of weak discontinuities for $\delta > 0$ in planar van der Waals dusty gas flow. From Fig.3.2, we see that increasing the value of k_p

increases the time for the decay of weak discontinuities for $\delta > 0$. It is also noticeable that in the dust-free flow, the non-ideal parameter b accelerates the distortion of weak discontinuities for $\delta > 0$. Thus, the behavior of flow patterns of the weak discontinuities for $\delta > 0$ influenced by k_p is opposite with the behavior of the flow influenced by b. It is noticeable that the flattening of weak discontinuities for $\delta > 0$ in planar non-ideal gas flow is faster than the planar ideal gas flow. From Fig.3.2, it is clear that the van der Waals parameter b together with the mass fraction k_p enhance the rate of distortion of weak discontinuities for $\delta > 0$. Fig.3.3 depicts that the van der Waals parameter b in non-dusty medium accelerates the growth of the weak discontinuities for $\delta < 0$. It is found that an increase in the value of mass fraction k_p causes to slow down the growth of the weak discontinuities for $\delta < 0$ in planar ideal and non-ideal gas flow. Thus, the presence of dust particles delay the shock formation.

The decay of the weak discontinuities for $\delta > 0$ and growth of the weak discontinuities for $\delta < 0$, respectively for non-planar ($m = 1$) flow are shown in Fig.3.4 and 3.5, and the results obtained for the non-ideal dusty gas for cylindrically symmetric (non-planar with $m = 1$) flow are compared to the results obtained in ideal dusty gas flow. Flow patterns are the same in cylindrically symmetric flow as in the case of planar flow. In both cases, the van der Waals parameter b together with the mass fraction k_p enhances the time for the decay of weak discontinuities for $\delta > 0$ and reduces the time for shock formation.

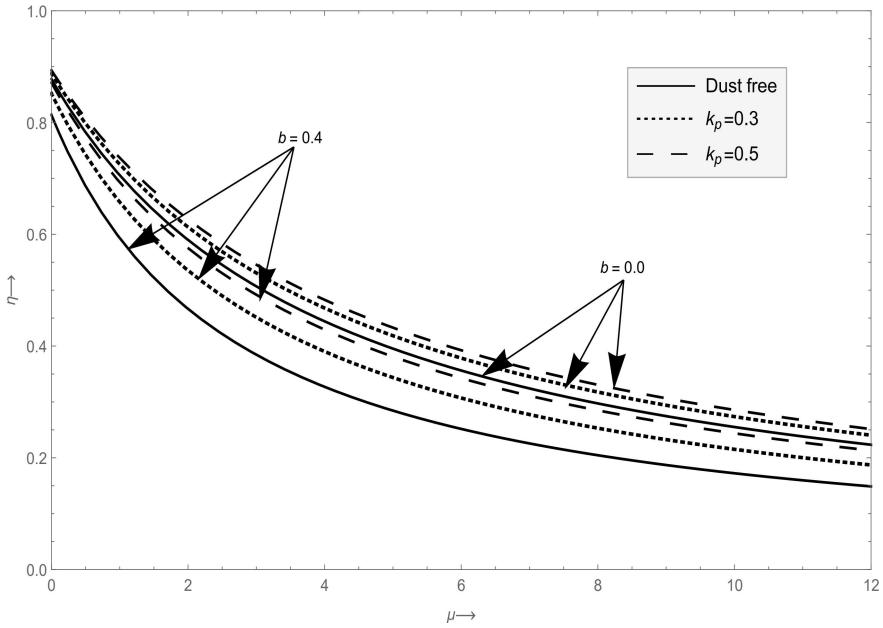

FIGURE 3.2: Effect of dust particles on the decay process of expansive weak discontinuities with $\beta = 0.8$, $\gamma = 1.67$ and $\delta = 0.1$ for planar symmetry.

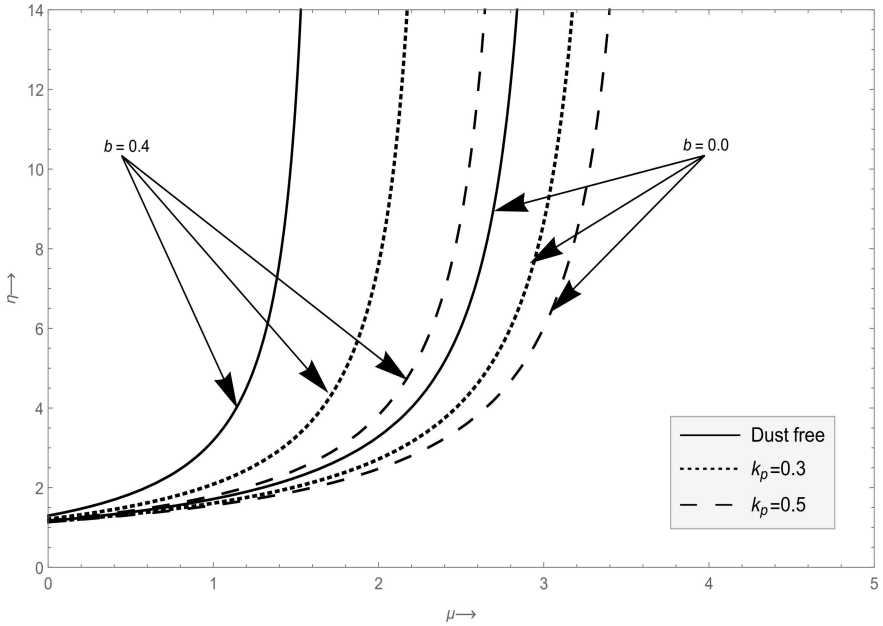

FIGURE 3.3: Effect of dust particles on the growth of compressive weak discontinuities with $\beta = 0.8$, $\gamma = 1.67$ and $\delta = -0.1$ for planar symmetry.

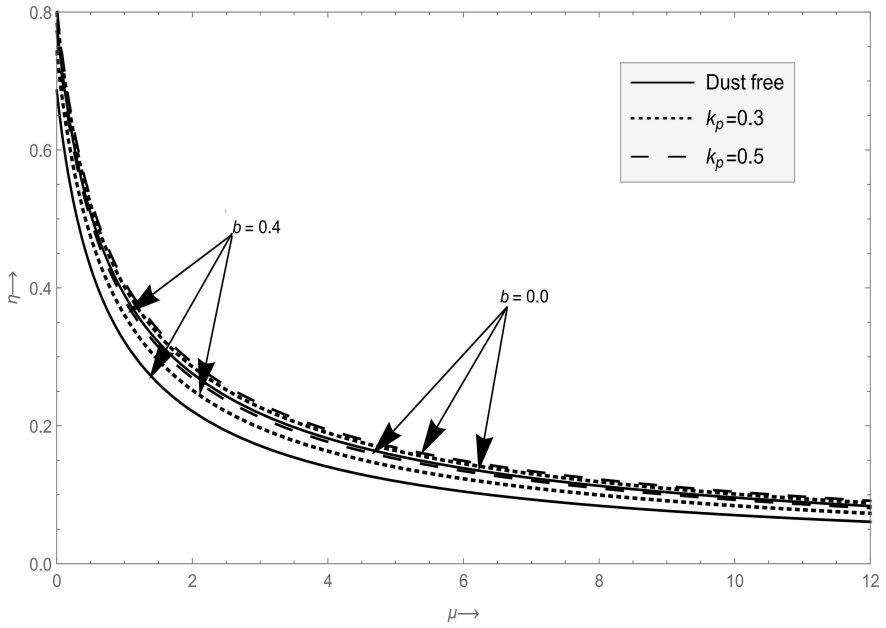

FIGURE 3.4: Effect of dust particles on the decay of expansive weak discontinuities with $\beta = 0.8$, $\gamma = 1.67$ and $\delta = 0.1$ for cylindrical symmetry ($m = 1$).

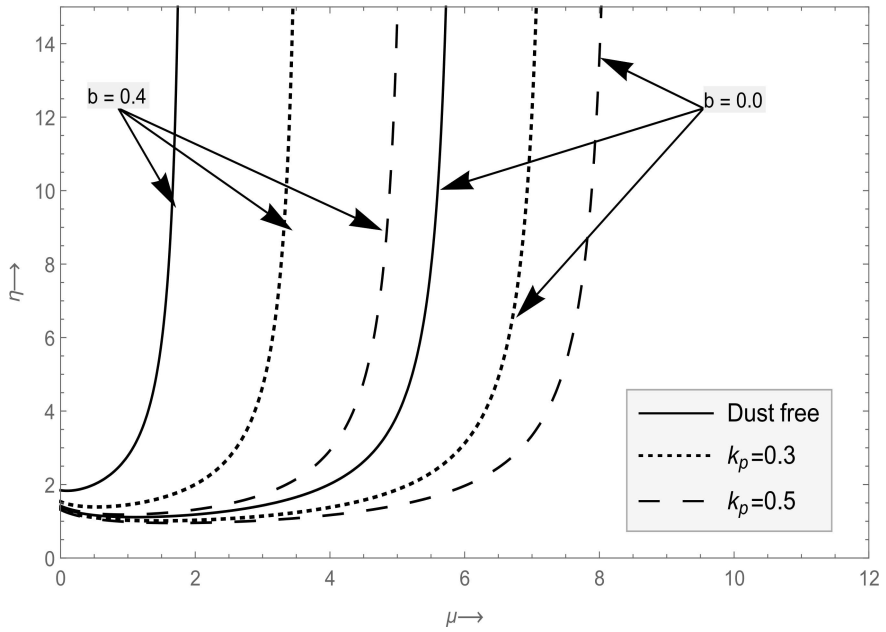

FIGURE 3.5: Effect of dust particles on the growth of compressive weak discontinuities with $\beta = 0.8$, $\gamma = 1.67$ and $\delta = -0.1$ for cylindrical symmetry ($m = 1$).

Now, we discuss the effect of van der Waals parameter b for distinct values ($b =$

$0.0, 0.1, 0.2, 0.3, 0.4$), where $b = 0$ corresponds to ideal gas, in the presence of the small solid dust particles for planar and cylindrically symmetric ($m = 1$) flow. The value of mass fraction of solid dust particles $k_p = 0.03$ corresponds to the dusty gas. The curves presented in Fig.3.6 show the non-idealness effect on the weak discontinuities for ($\delta > 0$) for planar flow and the curves presented in Fig.3.7 show the non-idealness effect on the growth of weak discontinuities for ($\delta < 0$) for planar flow. From Fig.3.6 it can be seen that if we increase the value of the van der Waals parameter b, then the process of decay for $\delta > 0$ increases and similarly from Fig.3.7, it is found that if we increase the value of non-ideal parameter b, then the growth process of the solution curve for $\delta < 0$ increases for planar flow in dusty medium. Also, it is observed that, for a fixed value of k_p, an increase in b enhances the rate of decay of weak discontinuities for $\delta > 0$.

Fig.3.8 and 3.9 shows the growth of the weak discontinuities for $\delta < 0$ and the decay of the propagating weak discontinuities for $\delta > 0$ for different values of non-ideal parameter b in non-planar dusty gas flow. Fig.3.8 and Fig.3.9, one can observe that the flow profile is similar for cylindrically symmetric ($m = 1$) flow as in the case of planar flow. Also, we observed that the increasing values of b accelerate the rate of decay of weak discontinuities for $\delta > 0$ and decreases the time for shock formation.

Now, we study the evolutionary behavior of weak discontinuities for both planar and non-planar ($m = 1$) cases in non-ideal dusty gas flow. Fig.3.10 and Fig.3.11 demonstrate a comparative analysis of weak discontinuities for $\delta > 0$ and $\delta < 0$ in planar and non-planar ($m = 1$) flows, respectively. From Fig.3.10, we see that the weak discontinuities for $\delta > 0$ take less time to decay in the case of cylindrically symmetric flow than the planar flow. Fig.3.11 shows that in the case of cylindrically symmetric flow, weak discontinuities for $\delta < 0$ takes more time to become shock than the planar flow. Also, we observe that the shock formation in planar non-ideal

dusty gas flow is faster as compared to the non-planar non-ideal dusty gas flow, i.e. the weak discontinuities for $\delta < 0$ in non-ideal dusty gas flow end up with the shock earlier in case of planar flow as compared to the non-planar flow ($m = 1$).

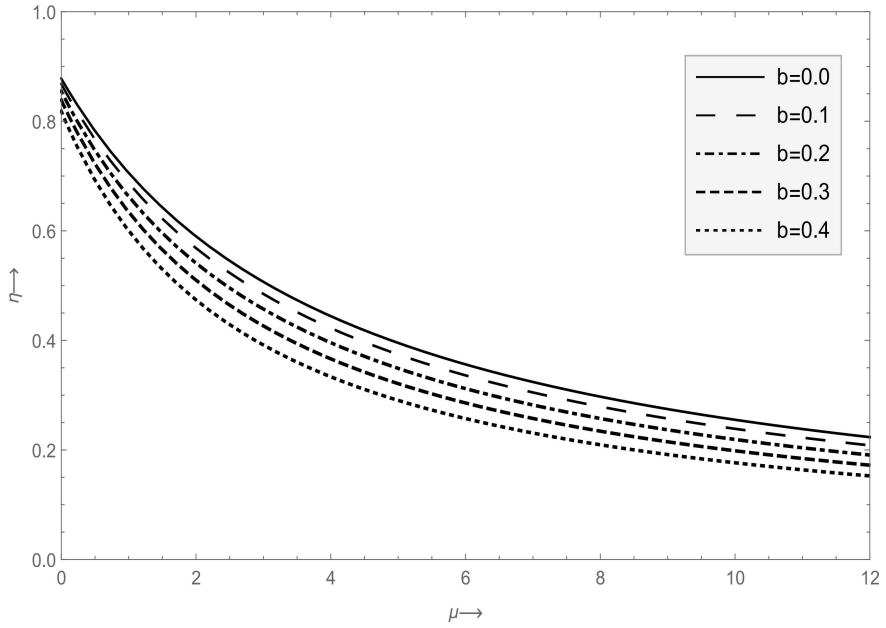

FIGURE 3.6: Effect of van der Waals parameter b on the decay of expansive weak discontinuities with $\beta = 0.8$, $\gamma = 1.67$, $k_p = 0.03$ and $\delta = 0.1$ for planar symmetry.

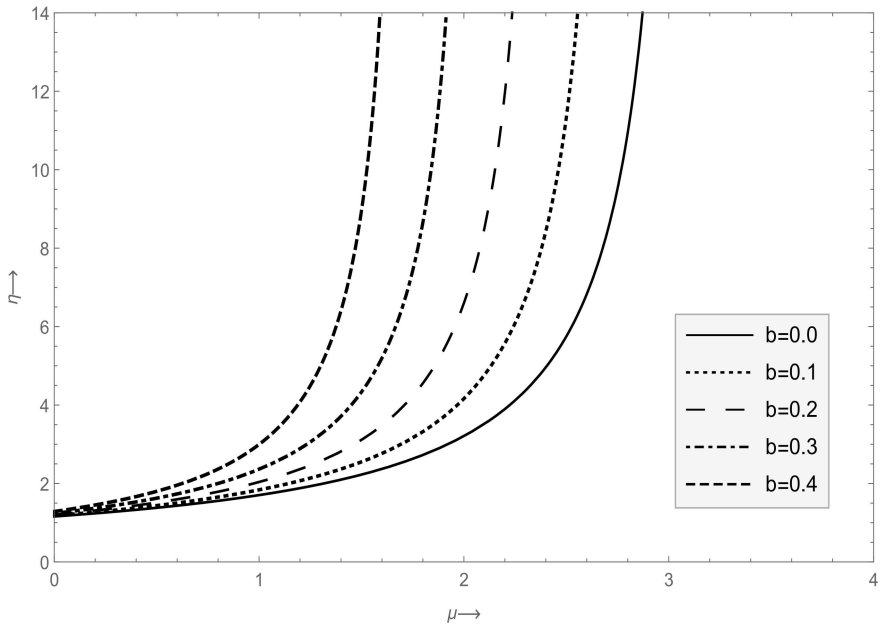

FIGURE 3.7: Effect of van der Waals parameter b on the growth of compressive weak discontinuities with $\beta = 0.8, \gamma = 1.67$, $k_p = 0.03$ and $\delta = -0.1$ for planar symmetry.

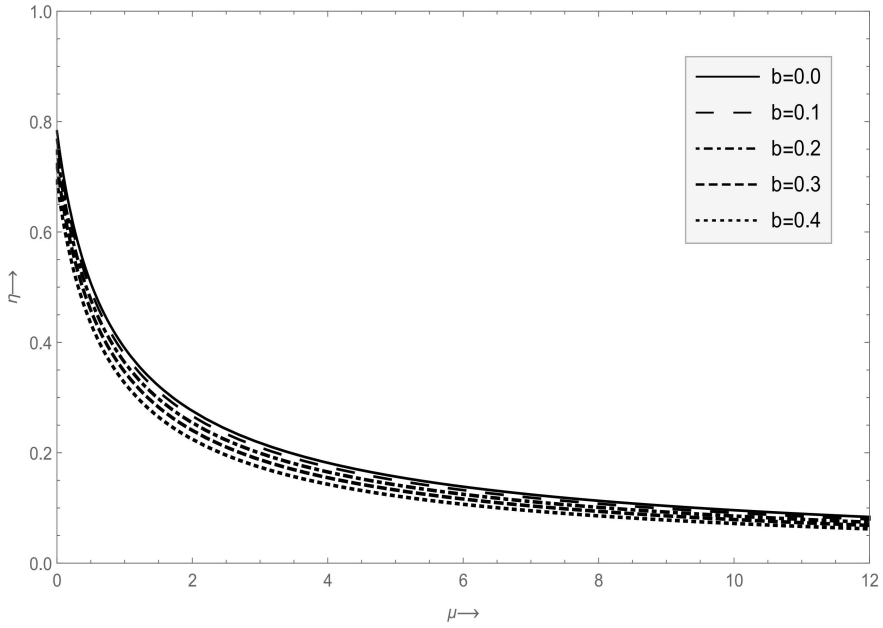

FIGURE 3.8: Effect of van der Waals parameter b on the decay of expansive weak discontinuities with $\beta = 0.8$, $\gamma = 1.67$, $k_p = 0.03$ and $\delta = 0.1$ for cylindrical symmetry ($m = 1$).

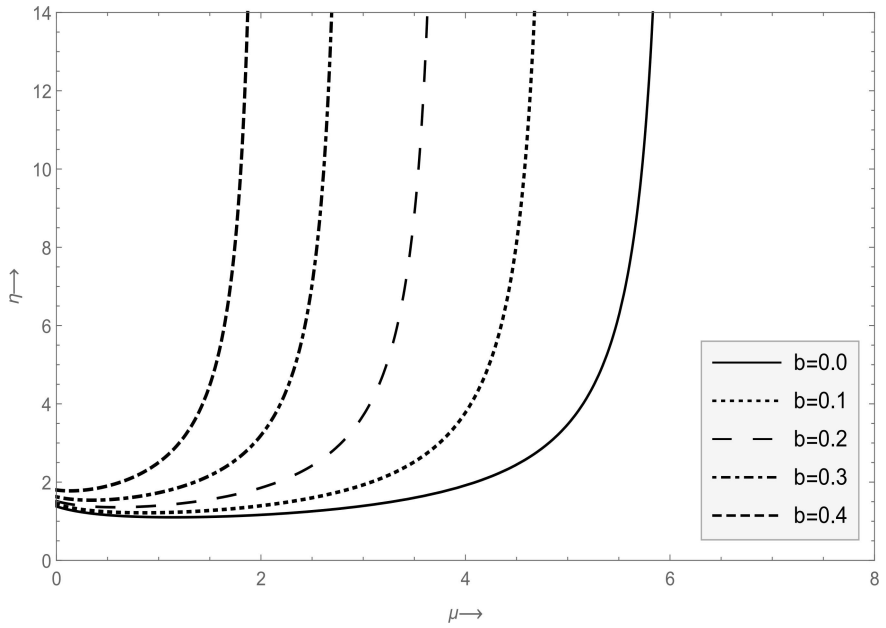

FIGURE 3.9: Effect of van der Waals parameter b on the growth of compressive weak discontinuities with $\beta = 0.8$, $\gamma = 1.67$, $k_p = 0.03$ and $\delta = -0.1$ for cylindrical symmetry ($m = 1$).

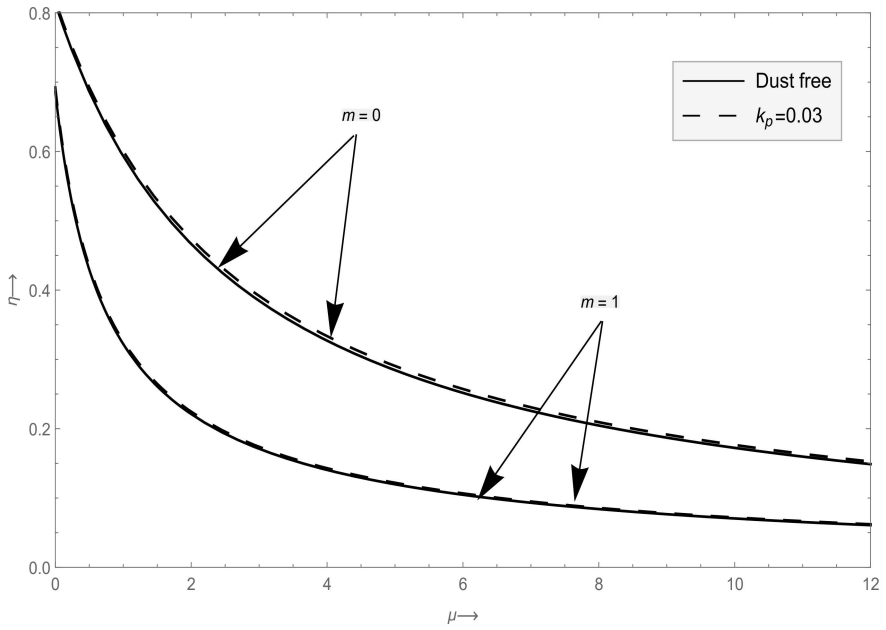

FIGURE 3.10: Effect of dust particles on the expansive weak discontinuities for planar and cylindrical symmetry ($m = 1$) dusty gas flow with $b = 0.4$.

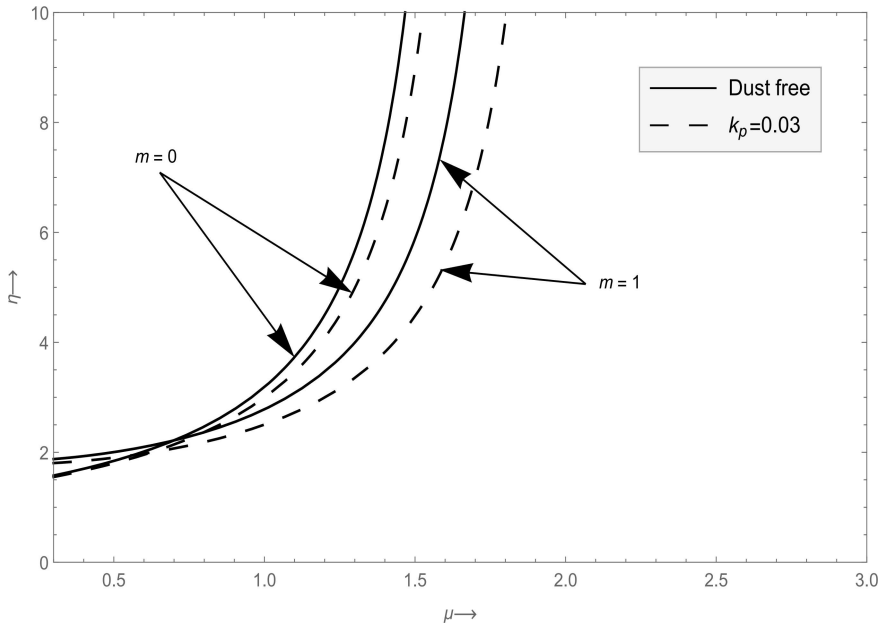

FIGURE 3.11: Effect of dust particles on the compressive weak discontinuities for planar and cylindrical symmetry ($m = 1$) dusty gas flow with $b = 0.4$.

3.6 Conclusion

This study examined the different parameter effects on the flow pattern of weak discontinuities in one-dimensional dusty van der Waals gas. The effect of the mass fraction of dust particles on the propagation of weak discontinuities with planar and non-planar van der Waals gas flow is studied. The shock formation condition is derived, and it is shown that after a finite distance of propagation, weak discontinuities for $\delta < 0$ become shock. The presence of solid particles in the medium increases the distortion rate of weak discontinuities for $\delta > 0$ and slows down the shock formation rate. Therefore, we see that the non-deal parameter and the mass fraction's combined effect accelerate the distortion of weak discontinuities for $\delta > 0$ and hasten the growth of the weak discontinuities for $\delta < 0$. It is observed that the weak discontinuities for $\delta > 0$, decay faster in planar flow than in non-planar flow and that the weak discontinuities for $\delta < 0$, transition to shock more quickly

in planar flow than in non-planar flow. Therefore, it is concluded that in both cases planar and non-planar flows, the presence of dust particles accelerate the rate of decay of weak discontinuities for $\delta > 0$ and also, reduces the time for shock formation in van der Waals gas. Thus, the behavior of the solution curves entirely relies on the parameter of non-idealness and the mass fraction of the dust particles in either case. It varies on the variation of the values of the parameters.

****